

Visualization of the Quality of Surfaces and Their Derivatives

K. Kraus

Abstract

Continuous geographic information, such as terrain elevations or temperature, can be represented either as vectors, e.g., isolines, or as raster, e.g., pixel graphics. This paper deals with the quality of these representations. Special attention is paid to the accuracy of secondary information, such as terrain slopes, derived from digital elevation models. For a mathematical analysis, synthetic surfaces are employed. In analyzing reality, surfaces and their derivatives are considered to be affected by random errors. As a conclusion, new ways of how to visualize the equality of surfaces and of their derivatives are shown. Thus, the misuse of land-related data stored in geographic information systems can be considerably reduced.

Preliminary Remarks

Worldwide, much effort is being invested in data acquisition for geographic information systems (GISs). Until recently, little attention has been paid to the quality of geographic data stored in GISs and of derived products. Disregarding aspects of accuracy often results in misuses of geographic data (Beard, 1989).

This paper deals with land-related data which can be represented by a function of geographic coordinates. In other words, the value of the function, Z , depends on X and Y , i.e., $Z(XY)$. The mathematical form of function $Z(XY)$ is not considered here, but the function must be continuous. The first derivatives $Z'_x(XY)$ and $Z'_y(XY)$ may, however, show discontinuities. This means that the surface represented by $Z(XY)$ contains break lines.

Function $Z(XY)$ may describe any continuous variable such as temperature or terrain elevation. Without limiting generality, we can assume a special case of function $Z(XY)$ describing terrain elevations.

Many GISs have the capability to derive isolines from the function $Z(XY)$, i.e., $Z(XY) = \text{constant}$. Such isolines can be intersected with other data such as cadastral boundaries. Sometimes, isolines of different functions are intersected with one another. In these cases, accuracies specified in the form of standard deviations σ_z are of no use; rather, what is needed is the accuracy of the isolines in the XY -plane, i.e., σ_{zp} ¹. This accuracy can be obtained as

$$\sigma_{zp} = \sigma_z / \tan \alpha = \sigma_z^* \Delta Z_p / \Delta Z \quad (1)$$

where

¹By applying these accuracy characteristics, it becomes possible to derive the accuracy of those areas using formulae by Prisley *et al.* (1989).

Institut für Photogrammetrie und Fernerkundung, Gusshausstrasse 25-27/122, A-1040 Wien, Austria.

$\tan \alpha$ is the maximum terrain slope at a specific point, ΔZ is the isoline interval (usually constant over the entire area of interest), and ΔZ_p is the distance to the neighboring isolines in the XY -plane (ΔZ_p varies along the isoline).

We have to give careful consideration to the distance ΔZ_p of neighboring isolines. It may become very large. As a consequence, the standard deviation σ_{zp} of isolines may become very large, as well. Therefore, processes that depend on the intersection of isolines may yield bad or even unacceptable results. It has to be emphasized at this point that the above conclusion is valid for isoline information, i.e., $Z(XY) = \text{constant}$, in any form, either vector or raster.

The above problem will be examined in this paper from various view points. We start in the next section with the behavior of distances between neighboring isolines of analytical surfaces. In this context, derived surfaces are of special interest. In the final section, function $Z(XY)$ and its derivatives become stochastic variables; this means that we consider random errors σ_z , and create accuracy models for the GIS. That section also describes the visualization of these accuracy models.

Isolines of Analytical Surfaces

Figure 1 shows a set of analytical surfaces with contours. To the left there are two helicoidal surfaces; straight contours of the first surface intersect in point S_1 , and those of the second surface in point S_2 . In the center of this figure we show a cone of revolution with center point C of the contours. In the oblique plane intersecting the cone from the right, contours are parallel equidistant straight lines. The surface to the very right is a hyperbolic paraboloid; its contours are hyperbolas.

The distance ΔZ_p between neighboring contours is inversely proportional to the (terrain) slope, $\tan \alpha$. In horizontal surfaces the distance ΔZ_p of neighboring contours is infinitely large. A horizontal area of the surface with an elevation not equal to that of any contour cannot be represented by those lines. However, in the case of a horizontal area at the elevation of a contour, the corresponding contour covers the entire area, i.e., it is undefined as a line. In other words, for surfaces that incorporate horizontal areas, one has to deal with both lines and areas of equal (terrain) elevation.

The problem becomes more interesting if one considers lines and areas of equal (terrain) slope. For the analytical surfaces mentioned above, Figure 2 shows the slope-lines.

Photogrammetric Engineering & Remote Sensing,
Vol. 60, No. 4, April 1994, pp. 457-462.

0099-1112/94/6004-457\$03.00/0
©1994 American Society for Photogrammetry
and Remote Sensing

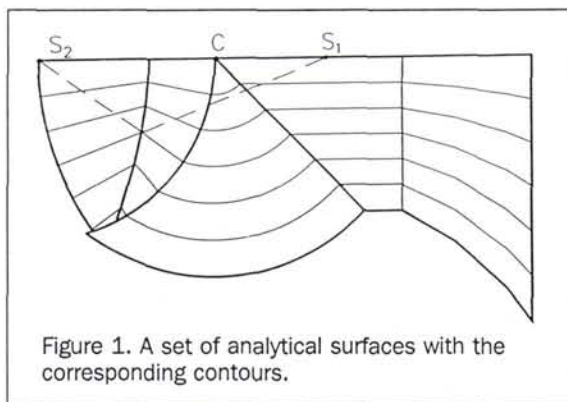


Figure 1. A set of analytical surfaces with the corresponding contours.

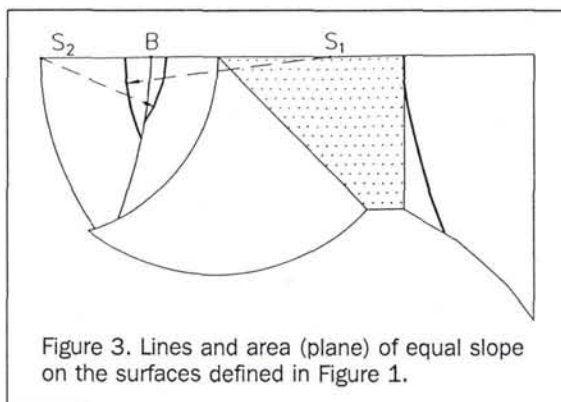


Figure 3. Lines and area (plane) of equal slope on the surfaces defined in Figure 1.

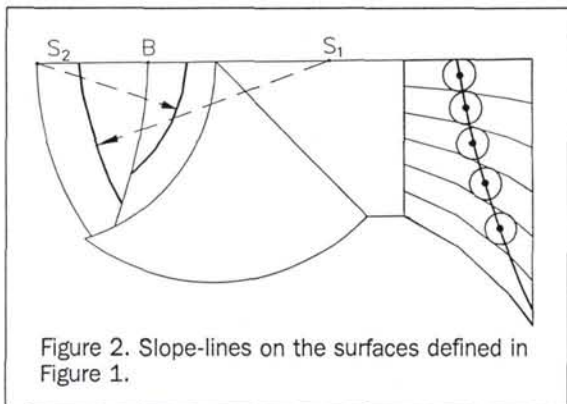


Figure 2. Slope-lines on the surfaces defined in Figure 1.

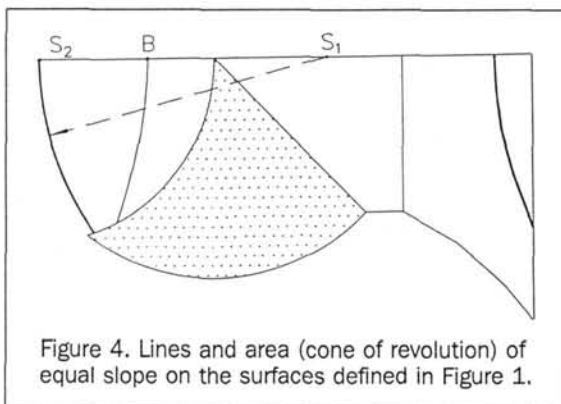


Figure 4. Lines and area (cone of revolution) of equal slope on the surfaces defined in Figure 1.

The slope value of the line is chosen to be smaller than that of the oblique plane, and larger than that of the cone of revolution. Figure 2 (the right part) illustrates a way of constructing slope-lines on a contour map. Circles with a diameter corresponding to the slope value sought are fitted in between neighboring contours. The line connecting the centers of the circles defines the slope-line (Killian and Kraus, 1992). We obtain three line sections. The one in the hyperbolic paraboloid is part of an ellipse². Line sections in both helicoidal surfaces on the left of the figure are circles with center points S_1 and S_2 . At breakline B there is a displacement. This phenomenon can be generalized in the following way: non-symmetry of contours on both sides of a breakline shows up as a displacement of slope-lines at the breakline.

In Figure 3, the spacing of isolines corresponds to the slope of the oblique plane, while in Figure 4 it corresponds to the slope of the cone of revolution. Figures 3 and 4 facilitate the following generalizations:

- In surfaces of constant maximum slope (planes, cones of revolution, ...) the distance ΔZ_p between neighboring slope-lines becomes infinitely large. The error of these isolines in the XY -plane becomes infinitely large, too.

- Should the slope of a surface of constant maximum slope be equal to that represented by an isoline of slope, then the slope-line is not defined within the area of this surface. The corresponding slope-line covers the entire area. Consequently, in surfaces that contain areas of constant maximum slope, one has to deal with both lines and areas of equal (terrain) slope.

Isolines Affected by Random Errors

Knowing the behavior of isolines in analytical surfaces helps us interpret their behaviour in natural surfaces. Isolines in natural surfaces are affected by random errors that are caused on the one hand by the roughness of the terrain, and on the other hand by data acquisition. In the next chapter, contours will be analyzed, followed by an analysis of slope-lines.

Contours Affected by Random Errors

In Figure 5, contours with an interval of 10 m are shown; they were derived from a digital elevation model (DEM). This DEM does not contain any horizontal areas, and therefore the derivation of contours does not cause any problems. The DEM consists of a rectangular grid with intermeshed breaklines (Kraus *et al.*, 1982).

There are numerous ways of expressing the vertical accuracy σ_z of contours (e.g., Li, 1982; Tempfli, 1980). In this paper we are not primarily interested in the vertical accuracy, but in the planimetric accuracy of the contours in the XY -plane. Therefore, we are going to apply a simple formula to express the vertical accuracy. This formula proved to be

²I am grateful for this information to Prof. Dr. Paukowitsch, of the Institute for Geometry at the Vienna University of Technology. He called my attention to the work of Burmester (1871) on "isophots" in analytical surfaces. Isophots correspond to lines of equal slope for the case of vertical lighting. In his publication, Burmester shows that isophots of hyperbolic paraboloids are ellipses.

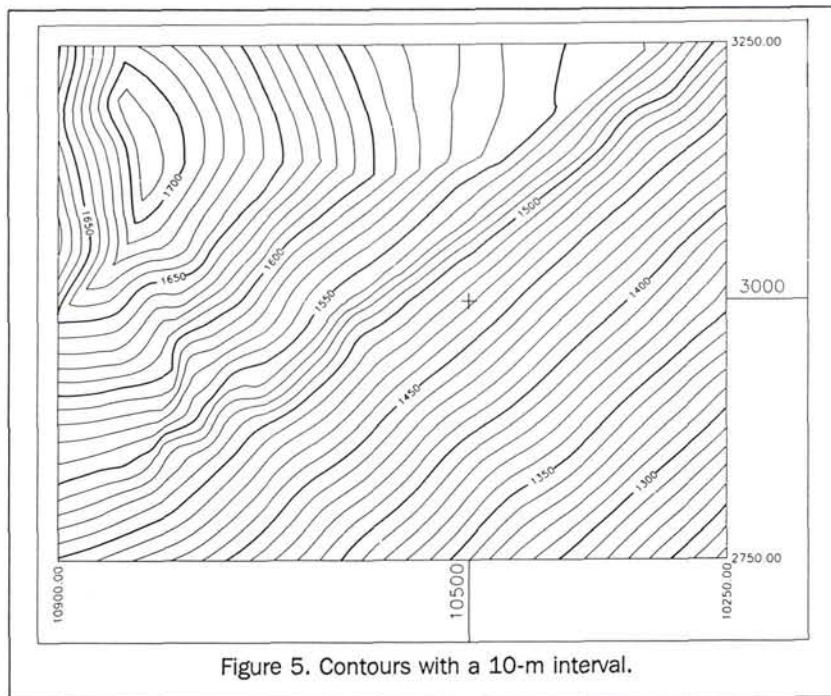


Figure 5. Contours with a 10-m interval.

adequate for describing the accuracy of contours derived from a DEM (e.g., Ackermann, 1978):

$$\sigma_z = a + b * Z' \tag{2}$$

where $Z' (= \tan\alpha)$ is the maximum slope at individual terrain points, coefficient b expresses the influence of the maximum terrain slope on height accuracy, and coefficient a denotes the component of the vertical accuracy that is independent of the maximum terrain slope. Thus, the two coefficients a and b describe the quality of products such as DEMs or contour maps, e.g., for the 1:5,000-scale German Base Map, $a = 0.4$ m and $b = 5$ m. There is an interdependence between coefficients a and b on the one hand, and flying height and image scale on the other hand (Kraus, 1987). Therefore, aerial photography can be planned in a way to correspond to pre-defined quality characteristics a and b .

However, as mentioned before, we are not interested in the vertical accuracy σ_z of points along contours but rather in the accuracy of these lines in the XY-plane σ_{zp} . This value can be derived using Equations 1 and 2: i.e.,

$$\sigma_{zp} = a / Z' + b. \tag{3}$$

For contours in Figure 5, estimates based on the flying height and the image scale yield (Kraus, 1987)

$$\sigma_{zp}[m] = (0.4 / Z') + 3. \tag{4}$$

According to this formula, the accuracy in the XY-plane at a terrain point with a slope of 100 percent is 3.4 m and, at a terrain point with 20 percent slope, 5.0 m. For the entire area of interest, σ_{zp} is visualized as a pixel graphic in Figure 6 with class boundaries 3.4 m (white), 3.8 m, 4.2 m, 4.6 m, and 5.0 m (black). The values of the terrain slope Z' for each pixel were derived from the DEM. The values Z' represent the inverse values of the distances ΔZ_p between neighboring contours.

In the future, GISs should include a model of accuracy

for the contours in the XY-plane, in addition to the DEM. Based on this model of accuracy, one could provide the positional accuracy of contours in the XY-plane at any point.

Slope-Lines Affected by Random Errors

In a DEM it is possible to derive the components of the normal vector to the terrain surface at each point of the rectangular grid, and at every intersection of a breakline with the grid (Kraus, 1987). The component of the normal vector along the maximum slope is used as the function value of the digital slope model (DSM). From this DSM the slope-lines can be derived. Figure 7 shows the slope-lines with an interval of 10 percent and the breaklines of the DEM displayed as bold lines. A comparison with the contours (Figure 5) concludes that

- There are displacements of varying size in the slope-lines along breaklines, and
- The distances ΔS_p between neighboring slope-lines become very large in areas of constant terrain slope.

The area of the terrain with elevations below 1450 m shows a fairly constant slope of 70 percent. The position of the isolines of slope in this area is more or less arbitrary. Given the arguments in the last section, one can easily detect a high degree of uncertainty in these lines. A raster image with a threshold of 70 percent would yield in this area a so-called "salt-and-pepper" pattern.

The uncertainty in slope-lines can be well visualized as a band of corresponding width at both sides of the slope-lines. The borders of these bands can be derived from the DSM as isolines of equal slope, e.g., for a slope-line of 70 percent at 69 percent and at 71 percent. In this example, the bandwidth corresponds to ± 1 percent. The bandwidth varies with the curvature of the terrain surface. In raster graphics, pixels within the band could be painted black, and all other pixels outside the band white. Figure 8 is such an image representing the bands of slope with a bandwidth of ± 1 per-

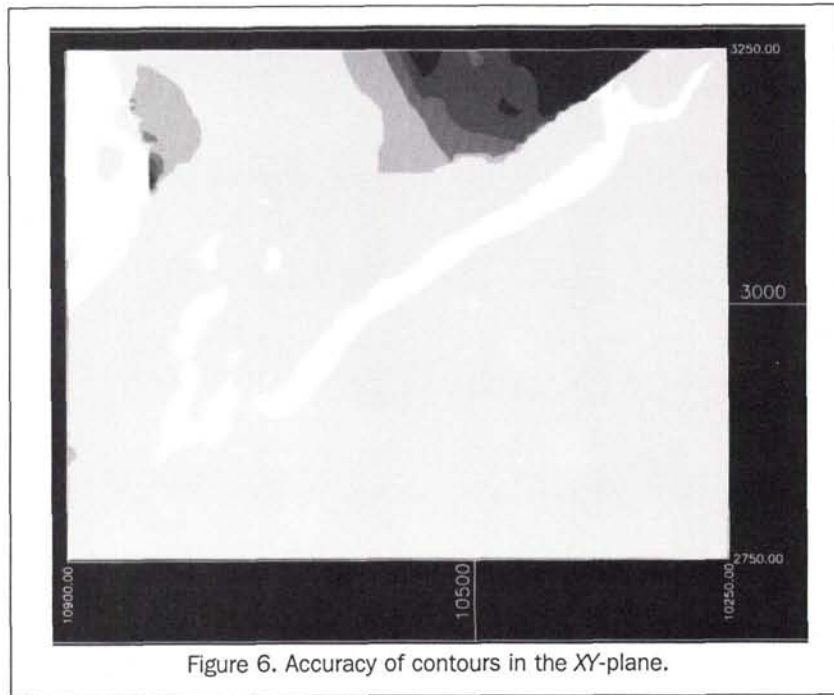


Figure 6. Accuracy of contours in the XY-plane.

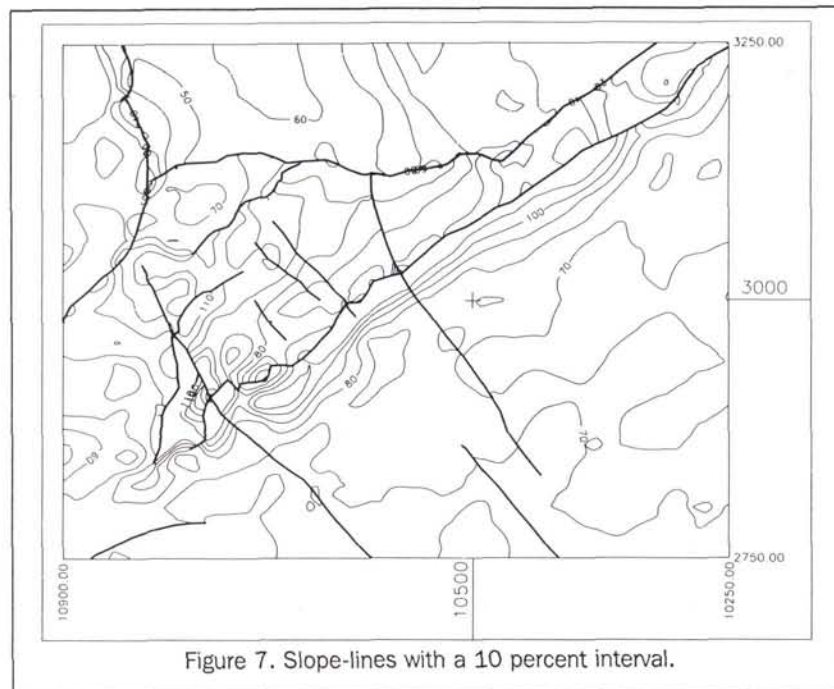


Figure 7. Slope-lines with a 10 percent interval.

cent. Variations in the width of the bands visualize the uncertainty of the position of the slope-lines. Overlaying these bands with the vector graphics (Figure 7) is of great value to GIS users.

This accuracy overlay can be made even more impressive, as shown in Figure 9. It shows the probability of the position of the lines in the XY-plane in correspondence with the Gaussian distribution. Gray shades in Figure 9 are ob-

tained as a sequence of overlapping bands along the slope-lines. To derive the borders of the bands in the sequence, a series of percentages was used that correspond to a Gaussian distribution, and to a standard deviation. Empirical studies have shown that $\sigma_s = \pm 1.5$ percent is an adequate value for the standard deviation. The black band corresponds to ± 0.375 percent, representing one-quarter of the standard deviation σ_s . Further values in this series were obtained as

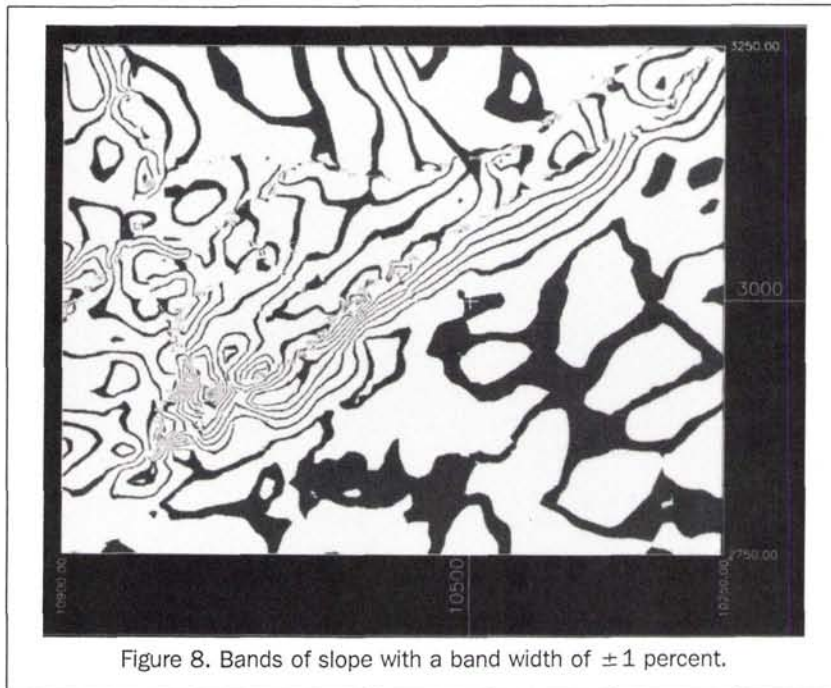


Figure 8. Bands of slope with a band width of ± 1 percent.

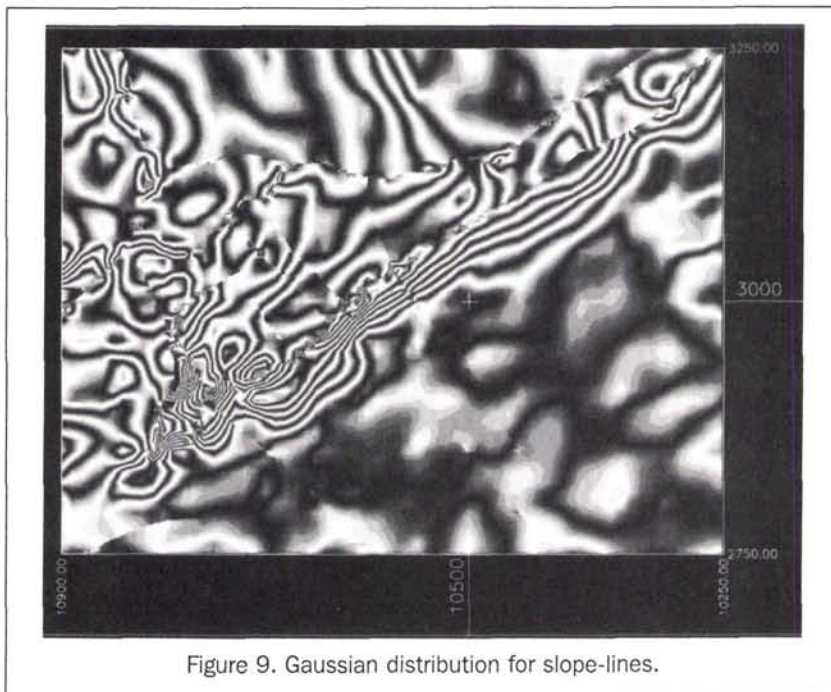


Figure 9. Gaussian distribution for slope-lines.

± 0.75 percent ($= \sigma_s/2$), ± 1.125 percent ($= 3\sigma_s/4$), ± 1.5 percent ($= \sigma_s$), ± 1.875 percent ($= 5\sigma_s/4$), etc. Tables of the Gaussian distribution can be found in many books on statistics. Using them, one can state the probability of the position of the slope-lines in the XY -plane. Within the black band this probability equals 20 percent. Further bands represented by lighter gray shades correspond to probabilities of 38 percent, 55 percent, 68 percent, 79 percent, and so on.

Similar to creating a model for the horizontal accuracy of contours of a DEM, a model for the horizontal accuracy of the slope-lines can be established for a DSM. There are only a few references to the accuracy of terrain slope values derived from DEMs. The following is based upon Equation 2:

$$\sigma_s = c + d * Z'' \quad (5)$$

where Z'' is the maximum slope of the surface as defined by the slope-lines, coefficient d expresses the influence of terrain curvature on the accuracy of the terrain slope values, and coefficient c denotes the component of slope accuracy which is independent of terrain curvature. Determining values for these coefficients will be the subject of extensive empirical studies in the future.

For the model of accuracy of slope-lines, the value σ_{sp} is necessary to express the accuracy in the XY -plane. This value can be obtained from considering Equations 1 and 5: i.e.,

$$\sigma_{sp} = c / Z'' + d. \quad (6)$$

Lacking well-based values for coefficients c and d , we are forced to omit any visualization of models of the accuracy of slope-lines in the XY -plane. It should be stressed, however, that future GISs should provide a model of accuracy for lines of equal slope in addition to the DSM. For this purpose, the second derivative Z'' at each terrain point is needed. These values are obtained as "slopes of slopes," i.e., subjecting the model with the first derivatives Z' , being the DSM, to a second process of derivation.

Conclusion

GISs must be extended to contain models that represent both geographic data and their quality. Information systems should yield both the value of a function and its accuracy. GIS users have to be informed about the accuracy of all direct and derived products of the system. Accuracy models must be visualized in a graphic form so that they can be easily interpreted and understood by the user. In this way, the misuse of geographic data yielded by GISs can be reduced considerably.

Acknowledgment

Examples for this paper have been created by Dr. K. Pyka, Institute for Geodesy, Technical University Cracov, Poland, during his time as a visiting researcher at the Institute for Photogrammetry and Remote Sensing of The Vienna Univer-

sity of Technology. He compiled the examples using SCOP (Sigle *et al.*, 1992), a program package for DEMs. The text has been translated from German to English by Dr. L. Molnar, The Vienna University of Technology, and Dr. K. Novak, The Ohio State University. My special thanks to the three reviewers (unknown to me). Their comments resulted in substantial improvements of this text.

References

- Ackermann, F., 1978. Experimental Investigation into the Accuracy of Contouring from DTM. *Photogrammetric Engineering*, 44(12):1537-1548.
- Beard, K., 1989. Use Error: the Neglected Error Component. *Proceedings AutoCarto 9*, Baltimore, 2-7 April, pp. 808-817.
- Burmester, L., 1871. *Theorie und Darstellung der Beleuchtung gesetzmaessig gestalteter Flaechen*. Verlag Teubner, Leipzig.
- Killian, K., and K. Kraus, 1992. Punkte in topographischen Flächen mit gleicher Geländeneigung. *Österreichische Zeitschrift für Vermessungswesen und Photogrammetrie*, 80(1):20-24.
- Kraus, K., E. Assmus, A. Köstli, L. Molnar, and E. Wild, 1982. Digital Elevation Models: Unser's Aspects. *Proceedings of the 38th Photogrammetric Week at Stuttgart University*, Copy 8:165-182.
- Kraus, K., 1987. *Photogrammetrie*. Band 2, Dmmler Verlag, Bonn, Germany.
- Li, Z., 1992. Variations of the Accuracy of Digital Terrain Models with Sampling Intervals. *The Photogrammetric Record*, 14(79):113-127.
- Prisley, S., T. Gregoire, and J. Smith, 1989. The Mean and Variance of Area Estimates Computed in an Arc-Node Geographic Information System. *Photogrammetric Engineering & Remote Sensing*, 55(11):1601-1612.
- Sigle, M., O. Hellwich, and A. Köstli, 1992. Intersection and Combination of Digital Elevation Models - Methods and Applications. *International Archives of Photogrammetry and Remote Sensing*, Washington, Volume 29, Part B4, Commission IV:pp. 878-882.
- Tempfli, K., 1980. Spectral Analysis of Terrain Relief for the Accuracy Estimation of Digital Terrain Models. *ITC-Journal* 1980(3):478-510.

(Received 21 July 1992; revised and accepted 14 January 1993; revised 16 February 1993)

Proceedings:
SPACE IMAGERY AND
NEWS GATHERING FOR
THE 1990s: SO WHAT?
Symposium on Foreign Policy
and Remote Sensing



Space Imagery and News Gathering for the 1990s: So What?

Gather valuable information by reading these proceedings from a Symposium on Foreign Policy and Remote Sensing, held 24-25 February 1989, at the Patterson School of Diplomacy and International Commerce, University of Kentucky.

Subjects covered: legal and national security implications of using space imagery; Congress and its role; human factor constraints on using space imagery; broadcasting and journalism perspective; and technological availability of space imagery.

1991. 121 pp. 4 colorplates. \$60 (softcover); ASPRS Members \$35. Stock # 4521.

For ordering information, see the ASPRS Store in this issue.